IEEE Access
Multidisciplinary | Rapid Review | Open Access Journal

Received May 2, 2018, accepted May 31, 2018, date of publication June 19, 2018, date of current version July 12, 2018.

Digital Object Identifier 10.1109/ACCESS.2018.2849016

Non-Invasive Assessment Model of Liver Disease Severity by Serum Markers Using Cloud Computing and Internet of Things

NAIPING LI[1], YONGFANG JIANG[1], GUOZHONG GONG[1], GUANGJIE HAN[2,3], (Member, IEEE), AND JING MA[1]

[1]Department of Infectious Disease, Second Xiangya Hospital, Central South University, Changsha 410007, China
[2]Department of Information and Communication System, Hohai University, Changzhou 213022, China
[3]State Key Laboratory of Acoustics, Institute of Acoustics, Chinese Academy of Sciences, Beijing 100190, China

Corresponding author: Guozhong Gong (gongguozhong@csu.edu.cn)

This work was supported by the National Natural Science Foundation of China under Grant 81730064 and Grant 81500455.

ABSTRACT Information on the stage of liver fibrosis is essential for decisions on antiviral treatment for chronic hepatitis B virus (HBV). This paper aims to establish a non-invasive assessment model with serum markers using cloud computing and the Internet of Things for the evaluation of liver disease severity and its prognosis. Based on the Internet of Things, the multiple and key information system of liver fibrosis or cirrhosis are constructed using the serum markers data. In the cloud platform, the probability density functions of indexes are used to select the optimized indicators. The logistic regression is used to establish the non-invasive assessment model. The patients were selected with CHB and underwent liver biopsy in the Second Xiangya Hospital, Central South University. There are two inclusion criteria: first, the patient received a liver biopsy according to ''Proclaim Prevention and Cure Guide For Chronic Hepatitis B'' of Chinese Medical Association in 2015; second, the patient has a history of hepatitis B or HBV surface antigen (HBsAg) positive more than six months, and HBsAg and (or) HBV DNA is still positive. Results of clinical data applications show that the accuracy of the non-invasive assessment model reaches greater than 70% for the recognition of significant liver fibrosis. In addition, the discriminant accuracy can be improved by increasing the number of indicators. The established non-invasive assessment model can be used for auxiliary clinical diagnosis after the further validation.

INDEX TERMS Non-invasive assessment, cloud computing, serum markers, liver disease severity.

I. INTRODUCTION

Chronic hepatitis B virus (HBV) infection affects an estimated 257 million individuals worldwide and about one million people chronically infected with HBV die from chronic liver diseases(including cirrhosis and hepatocellular carcinoma) in 2015 [1]. Many experimental and clinical literature data published in the last decade have indicated that liver fibrosis even earlier cirrhosis may be reversible [2]–[4]. Therefore, it is essential for the prognostication and decisions on antiviral treatment to identify the stage of liver fibrosis. Liver biopsy remains the gold standard for assessing the stages of liver fibrosis. Although liver biopsy is a safe procedure, it also has several disadvantages such as sampling error, poor patient compliance, the risk of poorly standardized collection of the liver tissues, limited usefulness for dynamic surveillance and follow-up, as well as poor observation concordance [5]–[9]. With all these limitations, accurate and reliable non-invasive predictors of histology are desperately needed to assess the hepatic fibrosis. Many studies have been performed using the readily available laboratory test results to predict significant fibrosis or cirrhosis [10]–[16].

Fibroscan is a non-invasive, painless, rapid (<5 min), and reproducible method for measuring liver stiffness with no complications. It cannot only be used for non-invasive diagnosis of liver fibrosis and monitoring the progress of liver disease, but also evaluating the effects of antiviral therapy or anti-fibrosis treatment. However, in overweight and obese patients (BMI>28), Fibroscan is unable to obtain results because the fatty thoracic belt attenuates both elastic waves and ultrasound. In addition, the large blood vessels in the liver will likely to lead to the incorrect results, so the great vessels structure needs to be avoided at diagnosis. Ascites is

TABLE 1. The non-invasive predictors of histology for discriminating significant fibrosis or cirrhosis.

NO	Methods	Indicators	Classification	Refs
1	Fibroscan: Uses both ultrasound (US) (5 MHz) and (50 Hz) elastic waves;propagation velocity	Instantaneous elastic spectrum of the liver	Significant fibrosis (>/= F2) and cirrhosis (= F4)	[10]
2	Fibro-test:logistic regression, neural connection, and ROC curves.	Alpha2 macroglobulin, alpha2 globulin (or haptoglobin), gamma globulin, gamma,apolipoproteinA1, glutamyltranspeptidase, and total bilirubin	High positive predictive value (>90% certainty of presence of F2, F3, or F4)	[11]
3	APRI: AST to platelet ratio index	AST, and platelet	Significant fibrosis and cirrhosis	[12]
4	Forns Index: a multivariate forward stepwise logistic regression analysis	Age, GGT, cholesterol, and platelet count	Discriminate with and without significant liver fibrosis	[13]
5	FibroSpect Ⅱ : Correlation analysis by Pearson and Spearman rho tests.	Hyaluronic acid, serum tissue inhibitor of metalloproteinase-1, and α-2-macroglobulin	Discriminate no, minimal and advanced fibrosis	[14]
6	European Liver Fibrosis Group: Scheuer D and Ishak D,statistical analysis	LN, age, HA,PIIINP,andTIMP-1	Fibrosis (sensitivity, 90%) and the absence of fibrosis	[15]
7	FPI: multiple logistic regression analysis identified	Age, aspartate aminotransferase (AST), total cholesterol level, insulin resistance, past alcohol intake	Mild (stages F0 or F1) or significant (stages F2-F4)	[16]
8	ShanghaiLiver Fibrosis Group: Multivariate analysis	Alpha2-macroglobulin, age, gamma glutamyl transpeptidase, and hyaluronic acid	With and without significant fibrosis	[5]

a physical limitation to the Fibroscan application [17]. For the hepatitis patients with acute liver damage, Fibroscan will overestimate the real stage of liver fibrosis [18]. Cholestasis and total bilirubin increased liver stiffness measurement value [19].

The non-invasive predictors of histology for discriminating significant fibrosis or cirrhosis were summarized in Table 1. Through statistical analysis, these comprehensive serum models were established using one or more specific indexes. The common characteristic is that the AUC is greater than 0.7, and its detection is obtained from clinical practice, which performs well in the diagnostic aspects of accuracy, sensitivity, specificity, positive predictive value, and negative predictive value. However, the unified comprehensive model for evaluating the degrees of fibrosis and inflammatory activity is scarce currently.

Therefore, it is very important to develop a comprehensive model considering multiple serum indicators, which characterized by safety rapidity and repeatability. This model is expected to dynamically evaluate and monitor the progress of chronic liver fibrosis, and especially it can provide an alternative to the liver biopsy in the follow-up visit.

In recent years, the internet of things [20], [21] and cloud computing [22]–[24] technologies provide a good technical guarantee for the achievement of this goal. In view of this, in this paper, a non-invasive testing system with serum makers using cloud computing and internet of things were established. The multiple information is used to evaluate the liver disease severity and its prognosis. In the data collect layer, the serum markers such as the blood routine indexes are collected and uploaded through the internet of things. In the cloud computing layer, the probability density functions are applied to select the optimized indicators, and the logistic regression is used to establish the non-invasive assessment model. In the non-invasive assessment layer, it is feasible to carry out the model optimization, evaluation of liver disease severity, and prognosis.

II. HIERARCHICAL STRUCTURE OF NON-INVASIVE ASSESSMENT SYSTEM USING CLOUD COMPUTING AND INTERNET OF THINGS FOR LIVER DISEASE SEVERITY

The hierarchical structure of the non-invasive assessment system is shown in Figure I, which composes of three layers: the data collect layer, the cloud computing layer, and the non-invasive assessment layer.

A. DATA COLLECT LAYER

This study was approved by the Clinical Research Committee of Second Xiangya Hospital, Central South University. Chronic HBV infection was diagnosed according to the guidelines published by the American Association for the Study of Liver Diseases in 2009 [25] and the latest ''Proclaim Prevention and Cure Guide for Chronic Hepatitis B'' from Chinese Medical Association in 2015 [26]. Cases with chronic HBV infection were included in this study if positive hepatitis B surface antigen (HBsAg) had been detected in the serum for at least 6 months or liver biopsies were evaluated by three senior pathologists in the Laboratory of Pathology, Second Xiangya Hospital. Cases were excluded from the study if biopsy evaluation showed no fibrosis. Patients diagnosed with chronic HBV infection but coinfected with HIV, hepatitis C virus, or hepatitis D virus were excluded from the study. The chronic HBV infected patients with the following diseases meanwhile were also excluded from this study, which are the nonalcoholic steatohepatitis, autoimmune liver diseases including autoimmune hepatitis, primary biliary cirrhosis, and primary sclerosing cholangitis, as well as hereditary and metabolic liver diseases such as Wilson's disease,

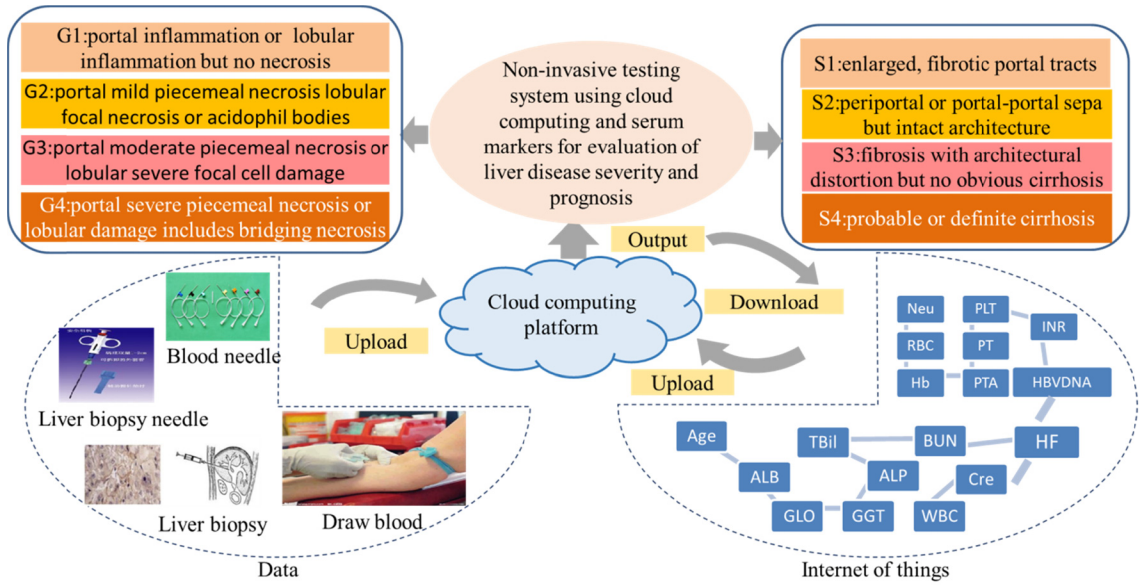

FIGURE 1. **The hierarchical structure of the non-invasive assessment system.Through the combination of data collect layer, cloud computing layer, and non-invasive layer, the liver disease severity and its prognosis can be evaluated and prognosticated.**

hemochromatosis, and α-1-antitrypsin deficiency. Patients with chronic HBV infection due to long-term exposure to toxic drugs and industrial toxicants, liver microcirculatory dysfunction, HCC, liver transplantation, and schistosomiasis need to be excluded from the study. Therefore, 1246 cases with chronic HBV infection were retrospectively recruited from March 2005 to December 2010 in the Department of Infectious Diseases, Second Xiangya Hospital. The serum markers of these cases can be collected and uploaded in the internet of things.

B. CLOUD COMPUTING LAYER

The cloud computing layer includes the selection of the optimized indicators and the establishment of non-invasive assessment model, which is the third layer of the non-invasive testing system. With the data transmitted from the internet of things, the important parameters including the key indicators and parameters of model can be solved through the cloud computing platform. Besides, these calculation results are also stored in this cloud computing platform, which means that the results can be downloaded from the platform whenever necessary. Therefore, a great convenience and sufficient data will be provided for decisions on antiviral treatment for chronic HBV.

C. NON-INVASIVE ASSESSMENT LAYER

The top layer of non-invasive assessment system is the test and application layer, which includes the model optimization, evaluation of liver disease severity, and prognosis. In this work, the output results of the liver disease severity from the cloud computing platform can be divided into two levels, which are the level 1 and the level 2. The level SL1 represents the degree of liver fibrosis as no significant liver fibrosis which was determined with S1 to S2. The level SL2 represents significant liver fibrosis with S3 to S4. The inflammation necrosis of G1 and G2 were classified as less severity GL1, and from G3 to G4 were classified as severity GL2.

III. NON-INVASIVE ASSESSMENT AND DISCUSSION

A. INDICATORS

The serum indicators are listed below, which are Hemoglobin(Hb), Red Blood Cells(RBC), White Blood Cells (WBC), Neutrophils(Neu), Platelets(PLT), Alanine Aminotransferase (ALT), Aspartate Aminotransferase (AST), Albumin (ALB), Globulin (GLO), Total Bilirubin (TBIL), Direct Bilirubin(DBIL), Total Bile Acid(TBA), prothrombin time activity percentage(PTA), international normalized ratio(INR), HBsAg, HBsAb, HBeAg, HBeAb, HBcIgG, HBcIgM, and HBV-DNA.

All cases underwent liver biopsy after the admission were guided by the ultrasound. The length of the liver tissue specimen is not less than 1 cm, which contains at least 6 portal areas. The liver tissue will be processed successively by formaldehyde fixation, paraffin embedding, sectioning, conventional HE staining, and mesh dyeing. The fibrosis score of portal tract was graded by Knodell scoring system (Inflammatory necrosis grade from G1 to G4, degree of fibrosis stages from S1 to S4). Three pathology experts identify all the pathological images.

The correlation of multiple diagnostic indexes and the degree of fibrosis (S), as well as the correlation of multiple diagnostic indexes and the degree of inflammatory activity (G) were analyzed using ROC characteristic.

Based on the analyses of ROC characteristic curves, results show that the areas under ROC curves of 23 indicators,

including Sex, Age, Hb, RBC, WBC, Neu, PLT, ALT, AST, ALB, GLO, TBIL, DBIL, TBA, PTA, INR, HBsAg, HBsAb, HBeAg, HBeAb, HBcIgG, HBcIgM, and HBV-DNA, for the inflammatory activity recognition are 0.532, 0.683, 0.415, 0.431, 0.376, 0.437, 0.29, 0.629, 0.638, 0.336, 0.675, 0.655, 0.636, 0.607, 0.596, 0.596, 0.52, 0.521, 0.383, 0.603, 0.491, 0.498, and 0.418, respectively. The areas under ROC curves of 23 indicators, including Sex, Age, Hb, RBC, WBC, Neu, PLT, ALT, AST, ALB, GLO, TBIL, DBIL, TBA, PTA, INR, HBsAg, HBsAb, HBeAg, HBeAb, HBcIgG, HBcIgM, and HBV-DNA, for the identification degree of significant liver fibrosis are 0.543, 0.7, 0.41, 0.428, 0.379, 0.436, 0.284, 0.613, 0.627, 0.339, 0.683, 0.668, 0.644, 0.611, 0.611, 0.611, 0.49, 0.519, 0.364, 0.621, 0.462, 0.497, 0.393, and 0.394, respectively.

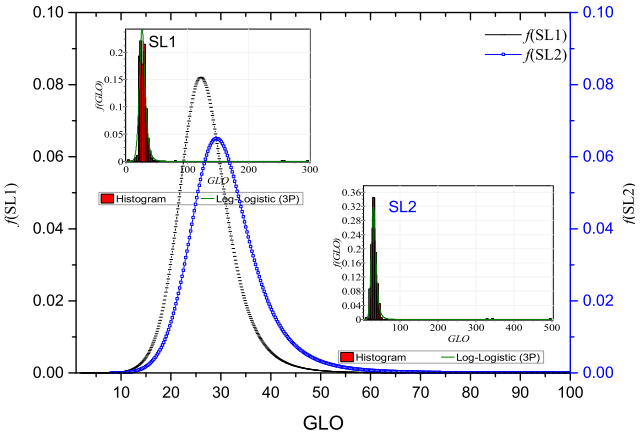

FIGURE 2. The probability density functions of GLO for the degree of liver fibrosis.

There are 12 indicators including Sex, Age, ALT, AST, GLO, TBIL, DBIL, TBA, PTA, INR, HBsAb, and HBeAb, where the areas for both the inflammation degree and significant liver fibrosis are greater than 0.5. The highest sensitivity index is GLO. The probability density functions of GLO for the identification of significant liver fibrosis were shown in Figure 2. It shows the probability density distributions of GLO for SL1 and SL2 are also different, where the peak values focus at 26 and 35, respectively.

B. NON-INVASIVE ASSESSMENT OF LIVER DISEASE SEVERITY BASED ON LOGISTIC REGRESSION IN CLOUD COMPUTING LAYER

The optimized indicators were selected as discriminant indexes and then the models were established using logistic regression. Logistic regression measures the relationship between a categorical dependent variable and one or more independent variables, which are usually (but not necessarily) continuous, using probability scores as the predicted values of the dependent variable. It is a statistical modeling technique in which the probability of a category is related to a set of explanatory variables. An explanation of logistic regression begins with a detailing of the logistic function, which always takes on values between zero and one. The logistic classification model is defined by the following equations:

$$Y = C_0 + C_1X_1 + C_2X_2 + C_3X_3 + \cdots + C_nX_n \quad (1)$$

$$P(Y) = \frac{e^Y}{1+e^Y} = \frac{1}{1+e^{-Y}} \quad (2)$$

Where Y is a measure of the contribution for the variables X_i $(i = 1, .., 6)$. C_i are the regression coefficients that are usually estimated using maximum likelihood estimation [27]–[29]. Unlike linear regression with normally distributed residuals, it is not possible to find a closed-form expression for the coefficient values that maximizes the likelihood function, so an iterative process must be used instead. $P(Y)$ is the categorical response of variables that represents the probability of a particular outcome. In present application, $C_1, C_2, C_3, \ldots, C_n$ are the coefficients of indicators including Sex, Age, Hb, RBC, WBC, Neu, PLT, ALT, AST, ALB, GLO, TBIL, DBIL, TBA, PTA, INR, HBsAg, HBsAb, HBeAg, HBeAb, HBcIgG, HBcIgM, and DNA. $P(Y)$ is the probability of a data point that tagged as a GL2/GL1/SL1/SL2. The threshold is 0.5, the record is regarded as a GL2/SL2 when $P(Y) > 0.5$, otherwise it is regarded as a GL1/SL1.

The discriminant function of logistic regression using the 12 selected indexes, including Sex, Age, ALT, AST, GLO, TBIL, DBIL, TBA, PTA, INR, HBsAb, and HBeAb, are listed in Table 2 B is the coefficient of the index. S.E. indicates the standard error around the coefficient for the constant. Wald and Sig. indicate the Wald chi-square test that tests the null hypothesis that the constant equals 0. This hypothesis is rejected because the p-value (listed in the column called "Sig.") is smaller than the critical p-value of 0.05 (or 0.01). Hence, we conclude that the constant is not 0. Exp(B) indicates the exponentiation of the B coefficient, which is an odds ratio. This value is given by default because odds ratios can be easier to interpret than the coefficient, which is in log-odds units. Through the established model, the classification results contain 565 GL1 and 310 GL2 samples. The correct classification accuracies are 81.2% and 56.7% for GL1 and GL2, respectively. The overall accuracy is 70.4%.

The discriminant functions of logistic regression using 23 indexes are listed in Table 3. A total of 552 GL1 and 344 GL2 samples are predicted using the classification model. The corresponding classification accuracies are 79.9% and 64.2%, respectively. The overall percentage is 73%. Althoughthe accuracy for GL1 decreases, the accuracy for GL2 and overall classification accuracy increase.

C. RESULTS AND DISCUSSIONS

Clearly, it can be seen that the overall classification accuracy of the logistic regression model with 23 indexes is higher than that with 12 selected indexes, which indicates that the accuracy can be improved by multiple indexes. The probability density functions were used to investigate the different characteristics of indicators for the degree of fibrosis (S) and the degree of inflammatory activity (G). The areas under ROC curves of PLT are 0.29 for the degree of inflammatory

TABLE 2. Variables of the logistic regression model using the 12selected indexes.

Indicators	B	S.E.	Wald	Sig.	Exp(B)	95% C.I.for EXP(B)	
						Lower	Upper
Sex	0.21	0.165	1.636	0.201	1.234	0.894	1.704
Age	0.048	0.006	59.351	0	1.049	1.036	1.062
ALT	0.000	0.001	0.23	0.632	1	0.999	1.001
AST	0.001	0.001	0.623	0.43	1.001	0.999	1.002
GLO	0.01	0.005	4.479	0.034	1.01	1.001	1.02
TBIL	-0.003	0.002	1.868	0.172	0.997	0.992	1.001
DBIL	0.004	0.004	1.204	0.273	1.004	0.997	1.012
TBA	0.012	0.003	16.029	0	1.012	1.006	1.018
PTA	-0.103	2.205	0.002	0.963	0.902	0.012	67.935
INR	3.807	27.576	0.019	0.89	45.027	0	1.34E+25
HBsAb	0.48	0.296	2.634	0.105	1.616	0.905	2.883
HBeAb	0.398	0.131	9.169	0.002	1.489	1.151	1.926
Constant	-5.241	0.56	87.662	0	0.005		

activity (G) and 0.284 for the degree of fibrosis (S), which is the minimum value in 23 indexes for both the degree of fibrosis and inflammatory activity. It indicates that PLT owns the least sensitivity for the degrees of fibrosis and inflammatory activity. The probability density functions of PLT for the inflammation degree were shown in Figure 3. It is clearly that the probability density distributions of PLT for GL1 and GL2 are different, and the peak values focus at 175 and 100, respectively. Thus, it can be indicated that PLT has different characteristics for GL1 and GL2. To compare the influence of PLT on discriminant accuracy, the parameters of logistic regression discriminant function using 12 selected indexes and PLT are calculated, which are listed in Table 4. Through the classification of 556 GL1 and 339 GL2 samples, the classification accuracies are 79.9% and 62% for GL1 and GL2, respectively. The overall classification accuracy is 72%. The results show that the overall accuracy is improved from 70.4% to 72%.

Since the probability densities may be different from the areas under the ROC curves. With very similar probability densities and smaller areas under the ROC curves, Hb and RBC were included in the models to investigate the accuracy change. The probability density functions of Hb and RBC for the inflammation degree were shown in Figures 4 and 5, respectively. The logistic regression discriminant function using selected 12 indexes, PLT, Hb, and RBC are calculated and listed in Table5.

Through the classification of 561 GL1 and 345 GL2 samples, the classification accuracies are 80.6% and 63.1% for GL1 and GL2, respectively. The overall accuracy is 72.9%. Obviously, the accuracies for GL1and GL2, as well as the overall accuracy increase, and the overall accuracy is improved from 70.4% to 72.9%. It means that the indicators Hb and RBC can also improve the discriminant accuracy, though they have very similar probability

TABLE 3. Variables of the logistic regression model using 23 indexes.

Indicators	B	S.E.	Wald	Sig.	Exp(B)	95% C.I.for EXP(B)	
						Lower	Upper
Sex	0.498	0.187	7.087	0.008	1.646	1.14	2.375
Age	0.040	0.007	33.479	0.000	1.041	1.027	1.055
Hb	-0.009	0.004	4.252	0.039	0.991	0.983	1
RBC	0.055	0.085	0.418	0.518	1.057	0.894	1.248
WBC	-0.034	0.037	0.85	0.356	0.966	0.898	1.039
Neu	-0.016	0.008	3.881	0.049	0.984	0.969	1
PLT	-0.008	0.001	48.513	0	0.992	0.99	0.994
ALT	0.000	0.001	0.083	0.774	1	0.999	1.001
AST	0.000	0.001	0.175	0.676	1	0.999	1.002
ALB	-0.052	0.01	24.826	0	0.95	0.93	0.969
GLO	0.008	0.005	3.352	0.067	1.009	0.999	1.018
TBIL	-0.002	0.002	1.215	0.27	0.998	0.993	1.002
DBIL	0.003	0.004	0.627	0.428	1.003	0.996	1.01
TBA	0.008	0.003	7.303	0.007	1.008	1.002	1.013
PTA	0.124	2.421	0.003	0.959	1.132	0.01	130.18
INR	0.469	30.289	0	0.988	1.598	0	9.67E+25
HBsAg	-0.096	0.281	0.116	0.733	0.909	0.524	1.577
HBsAb	0.085	0.33	0.066	0.797	1.088	0.571	2.076
HBeAg	-0.558	0.233	5.734	0.017	0.573	0.363	0.904
HBeAb	0.008	0.219	0.001	0.971	1.008	0.656	1.548
HBcIgG	-0.08	0.139	0.33	0.565	0.923	0.703	1.213
HBcIgM	-0.157	0.333	0.221	0.638	0.855	0.445	1.642
logDNA	-0.016	0.024	0.44	0.507	0.984	0.94	1.031
Constant	1.502	0.949	2.507	0.113	4.491		

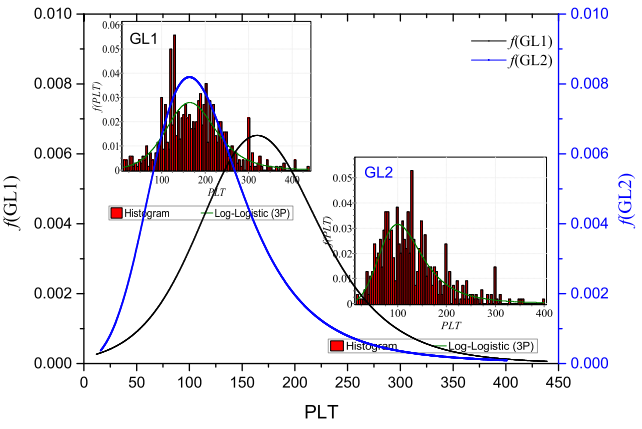

FIGURE 3. The probability density functions of PLT for the inflammation degree.

density distributions and smaller areas under the ROC curves between GL1 and GL2.

With very different probability density distributions between GL1 and GL2, as well as a smaller area under the ROC curve, ALB was included in the models to investigate the accuracy change. Figure 6 shows the probability density functions of ALB for the degree of fibrosis.

The logistic regression discriminant function of using 12 selected indexes, PLT, Hb, RBC, and ALB are calculated

TABLE 4. Variables of the logistic regression model using 12selectedindexes and PLT.

Indicators	B	S.E.	Wald	Sig.	Exp(B)	95% C.I.for EXP(B)	
						Lower	Upper
Sex	0.263	0.17	2.402	0.121	1.301	0.933	1.816
Age	0.038	0.006	35.9	0	1.039	1.026	1.052
ALT	0	0.001	0.066	0.798	1	0.999	1.001
AST	0.001	0.001	0.844	0.358	1.001	0.999	1.002
GLO	0.009	0.005	3.743	0.053	1.009	1	1.018
TBIL	-0.003	0.002	1.403	0.236	0.997	0.992	1.002
DBIL	0.006	0.005	1.673	0.196	1.006	0.997	1.016
TBA	0.01	0.003	11.676	0.001	1.01	1.004	1.016
PTA	0.718	2.29	0.098	0.754	2.051	0.023	182.321
INR	-7.034	28.639	0.06	0.806	0.001	0	2.10E+21
HBsAb	0.518	0.306	2.863	0.091	1.678	0.921	3.056
HBeAb	0.28	0.136	4.25	0.039	1.324	1.014	1.728
PLT	-0.009	0.001	66.197	0	0.991	0.989	0.993
Constant	-3.02	0.62	23.706	0	0.049		

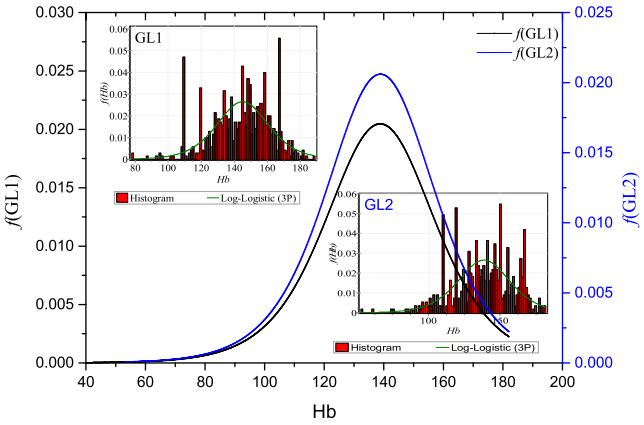

FIGURE 4. The probability density functions of Hb for the inflammation degree.

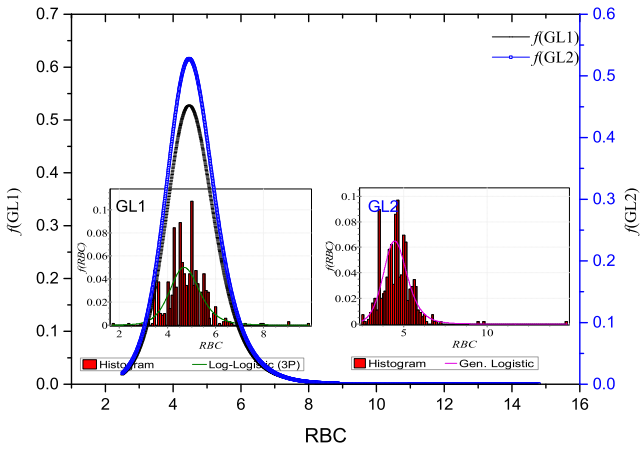

FIGURE 5. The probability density functions of RBC for the inflammation degree.

and listed in Table 6. Using the samples of 560 GL1 and 348 GL2, the classification accuracies are 80.5% and 63.6% for GL1 and GL2, respectively. The overall accuracy is 73%.

TABLE 5. Variables of the Logistic regression model using 12selected indexes, PLT, Hb, and RBC.

Indicators	B	S.E.	Wald	Sig.	Exp(B)	95% C.I.for EXP(B)	
						Lower	Upper
Sex	0.519	0.181	8.236	0.004	1.68	1.179	2.395
Age	0.04	0.007	38.359	0.000	1.041	1.028	1.055
ALT	0.000	0.001	0.001	0.974	1	0.999	1.001
AST	0.001	0.001	0.735	0.391	1.001	0.999	1.002
GLO	0.008	0.004	3.257	0.071	1.008	0.999	1.017
TBIL	-0.003	0.002	2.034	0.154	0.997	0.992	1.001
DBIL	0.004	0.004	1.179	0.278	1.004	0.997	1.012
TBA	0.01	0.003	10.804	0.001	1.01	1.004	1.015
PTA	0.127	2.316	0.003	0.956	1.136	0.012	106.419
INR	0.506	28.976	0	0.986	1.659	0	7.67E+24
HBsAb	0.33	0.311	1.124	0.289	1.391	0.756	2.56
HBeAb	0.296	0.138	4.607	0.032	1.344	1.026	1.761
PLT	-0.008	0.001	61.382	0	0.992	0.99	0.994
Hb	-0.017	0.004	19.586	0	0.983	0.976	0.991
RBC	-0.028	0.083	0.116	0.734	0.972	0.826	1.144
Constant	-0.873	0.793	1.213	0.271	0.418		

TABLE 6. Variables of the Logistic regression model using selected 12 indexes, PLT, Hb, RBC, and ALB.

Indicators	B	S.E.	Wald	Sig.	Exp(B)	95% C.I.for EXP(B)	
						Lower	Upper
Sex	0.514	0.183	7.91	0.005	1.672	1.169	2.393
Age	0.04	0.007	36.21	0	1.041	1.027	1.054
ALT	0	0.001	0.016	0.899	1	0.999	1.001
AST	0	0.001	0.233	0.63	1	0.999	1.002
GLO	0.008	0.005	3.054	0.081	1.008	0.999	1.017
TBIL	-0.003	0.002	2.22	0.136	0.997	0.992	1.001
DBIL	0.003	0.004	0.564	0.452	1.003	0.996	1.01
TBA	0.008	0.003	8.592	0.003	1.008	1.003	1.014
PTA	0.008	2.353	0	0.997	1.008	0.01	101.407
INR	2.044	29.432	0.005	0.945	7.723	0	8.72E+25
HBsAb	0.183	0.32	0.325	0.568	1.201	0.641	2.25
HBeAb	0.34	0.141	5.846	0.016	1.405	1.066	1.85
PLT	-0.008	0.001	56.734	0	0.992	0.99	0.994
Hb	-0.013	0.004	10.236	0.001	0.987	0.98	0.995
RBC	0.032	0.084	0.141	0.707	1.032	0.875	1.217
ALB	-0.053	0.01	27.084	0	0.948	0.93	0.968
Constant	0.559	0.845	0.437	0.509	1.748		

It shows the classification accuracy for GL1 decreases slightly, but the accuracy for GL2 and overall accuracy increase, where the overall percentage is improved from 70.4% to 73%. It can be clearly concluded that the overall discriminant accuracy can be improved by increasing the number of indicators.

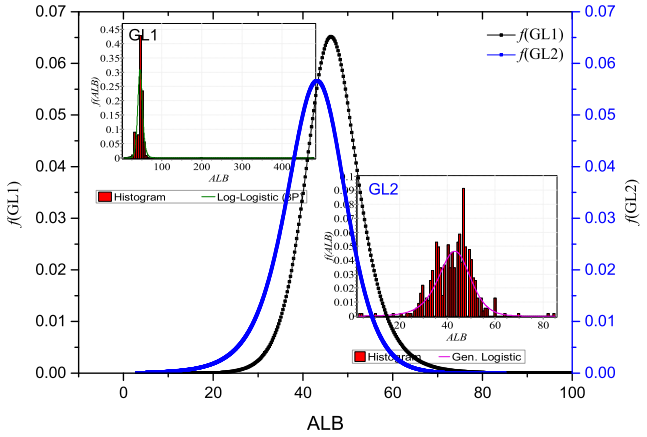

FIGURE 6. **The probability density functions of ALB for the inflammation degree.**

IV. CONCLUSIONS

A non-invasive assessment model of liver disease severity by serum markers using cloud computing and internet of things were established in this paper. It includes three layers: data collect layer, cloud computing layer, and non-invasive assessment layer. The correlation of multiple diagnostic indexes and the degree of fibrosis (S), as well as the correlation of multiple diagnostic indexes and the degree of inflammatory activity (G) were analyzed using ROC characteristic. 23 indicators including Sex, Age, Hb, RBC, WBC, Neu, PLT, ALT, AST, ALB, GLO, TBIL, DBIL, TBA, PTA, INR, HBsAg, HBsAb, HBeAg, HBeAb, HBcIgG, HBcIgM, and DNA are analyzed. The 12 indicators including Sex, Age, ALT, AST, GLO, TBIL, DBIL, TBA, PTA, INR, HBsAb, and HBeAb, where the areas for both the inflammation degree and significant liver fibrosis are greater than 0.5.The highest sensitivity index is GLO. Through the classification of 565 GL1 and 310 GL2 samples with the 12selected indicators,the classification accuracies are 81.2% and 56.7 for GL1 and GL2, respectively. The overall accuracy is 70.4%. Through the classification of 552 GL1 and 344 GL2 samples using 23 indexes, the classification accuracies are 79.9% and 64.2% for GL1 and GL2, respectively. Compared to that of the model with 12 indicators,the accuracy for GL1 decreases, but the accuracies for GL2 and the overall accuracy increase. Results from the probability density distributions and the areas under the ROC curves may be different. However, even the probability density functions of Hb and RBC are very similar between GL1 and GL2, they still can improve the discriminant accuracy. It also concludes that PLT has the least sensitivity for the degrees of fibrosis and inflammatory activity, but the classification results show that it can improve the overall accuracy from 70.4% to 72%. Through the data analysis and practical application, it is proved that the developed non-invasive assessment model of liver disease severity by serum markers using cloud computing and internet of things can not only achieve efficient classification for GL1 and GL2, as well as SL1 and SL2, but also calculate the G/S levels using the advantages of multiple indicators, which is a novel idea and an effective evaluation method for decisions on antiviral treatment for chronic HBV.

REFERENCES

[1] *Global Hepatitis Report 2017*, World Health Org., Geneva, Switzerland, Dec. 2017.

[2] D. Povero *et al.*, "Liver fibrosis: A dynamic and potentially reversible process," *Histol. Histopathol.*, vol. 25, no. 8, pp. 1075–1091, Aug. 2010.

[3] M. Pinzani, "Pathophysiology of liver fibrosis," *Digestive Diseases*, vol. 33, no. 8, pp. 492–497, Jul. 2015.

[4] E. Novo, S. Cannito, C. Paternostro, C. Bocca, A. Miglietta, and M. Parola, "Cellular and molecular mechanisms in liver fibrogenesis," *Arch. Biochem. Biophys.*, vol. 548, pp. 20–37, Mar. 2014.

[5] M. D. Zeng *et al.*, "Prediction of significant fibrosis in HBeAg-positive patients with chronic hepatitis B by a noninvasive model," *Hepatology*, vol. 42, no. 6, pp. 1437–1445, Dec. 2005.

[6] European Association for Study of Liver and Asociacion Latinoamericana para el Estudio del Higado, "EASL-ALEH clinical practice guidelines: Non-invasive tests for evaluation of liver disease severity and prognosis," *J. Hepatol.*, vol. 63, no. 1, pp. 237–264, Jul. 2015.

[7] J. F. Cadranel, P. Rufat, and F. Degos, "Practices of liver biopsy in France: Results of a prospective nationwide survey," *Hepatology*, vol. 32, no. 3, pp. 477–481, Sep. 2000.

[8] R. J. Fontana and A. S. F. Lok, "Noninvasive monitoring of patients with chronic hepatitis C," *Hepatology*, vol. 36, no. 5, pp. S57–S64, Nov. 2002.

[9] T. Poynard *et al.*, "Prospective analysis of discordant results between biochemical markers and biopsy in patients with chronic hepatitis C," *Clin. Chem.*, vol. 50, no. 8, pp. 1344–1355, Aug. 2004.

[10] L. Sandrin *et al.*, "Transient elastography: A new noninvasive method for assessment of hepatic fibrosis," *Ultrasound Med. Biol.*, vol. 29, no. 12, pp. 1705–1713, Dec. 2003.

[11] F. Imbert-Bismut, V. Ratziu, L. Pieroni, F. Charlotte, Y. Benhamou, and T. Poynard, "Biochemical markers of liver fibrosis in patients with hepatitis C virus infection: A prospective study," *Lancet*, vol. 375, no. 9262, pp. 1069–1075, Apr. 2001.

[12] C. T. Wai *et al.*, "A simple noninvasive index can predict both ignificant fibrosis and cirrhosis in patients with chronic hepatitis C," *Hepatology*, vol. 38, no. 2, pp. 518–526, Aug. 2003.

[13] X. Forns *et al.*, "Identification of chronic hepatitis C patients without hepatic fibrosis by a simple predictive model," *Hepatology*, vol. 36, no. 4, pp. 986–992, Oct. 2002.

[14] K. Patel *et al.*, "Correlation of FIBROSpect II with histologic and morphometric evaluation of liver fibrosis in chronic hepatitis C," *Clin. Gastroenterol. Hepatol.*, vol. 6, no. 2, pp. 242–247, Feb. 2008.

[15] W. M. C. Rosenberg *et al.*, "Serum markers detect the presence of liver fibrosis: A cohort study," *Gastroenterology*, vol. 127, no. 6, pp. 1704–1713, Dec. 2004.

[16] A. Sud *et al.*, "Improved prediction of fibrosis in chronic hepatitis C using measures of insulin resistance in a probability index," *Hepatology*, vol. 39, no. 5, pp. 1239–1247, May 2004.

[17] J. Foucher *et al.*, "Prevalence and factors associated with failure of liver stiffness measurement using FibroScan in aprospective study of 2114 examinations," *Eur. J. GastroenterolHepatol*, vol. 18, no. 4, pp. 411–412, Apr. 2006.

[18] A. Sagir, A. Erhardt, M. Schmitt, and D. Häussinger, "Transient elastography is unreliable for detection of cirrhosis in patients with acute liver damage," *Hepatology*, vol. 47, no. 2, pp. 592–595, Feb. 2008.

[19] G. Millonig *et al.*, "Extrahepatic cholestasis increases liver stiffness (FibroScan) irrespective of fibrosis," *Hepatology*, vol. 48, no. 5, pp. 1718–1723, Nov. 2008.

[20] D.-S. Xu, L.-J. Dong, L. Borana, and H.-B. Liu, "Early-warning system with quasi-distributed fiber optic sensor networks and cloud computing for soil slopes," *IEEE Access*, vol. 5, pp. 25437–25444, Nov. 2017.

[21] G. Han, W. Que, G. Jia, and W. Zhang, "Resource-utilization-aware energy efficient server consolidation algorithm for green computing in IIOT," *J. Netw. Comput. Appl.*, vol. 103, no. 2, pp. 205–214, Feb. 2018.

[22] L. Dong, W. Shu, D. Sun, X. Li, and L. Zhang, "Pre-alarm system based on real-time monitoring and numerical simulation using Internet of Things and cloud computing for tailings dam in mines," *IEEE Access*, vol. 5, pp. 21080–21089, Sep. 2017.

[23] G. Han, L. Liu, S. Chan, R. Yu, and Y. Yang, "HySense: A hybrid mobile crowdsensing framework for sensing opportunities compensation under dynamic coverage constraint," *IEEE Commun. Mag.*, vol. 55, no. 3, pp. 93–99, Mar. 2017.
[24] G. Han, L. Liu, W. Zhang, and S. Chan, "A hierarchical jammed-area mapping service for ubiquitous communication in smart communities," *IEEE Commun. Mag.*, vol. 56, no. 1, pp. 92–98, Jan. 2018.
[25] D. C. Rockey, S. H. Caldwell, Z. D. Goodman, R. C. Nelson, A. D. Smith, and American Association for the Study of Liver Diseases, "Liver biopsy," *Hepatology*, vol. 49, no. 3, pp. 1017–1044, Mar. 2009.
[26] J. J. Hou *et al.*, "Guideline of prevention and treatment for chronic hepatitis B (2015 update)," *J. Clin. Transl. Hepatol.*, vol. 5, no. 4, pp. 297–318, Nov. 2017.
[27] L.-J. Dong, J. Wesseloo, Y. Potvin, and X.-B. Li, "Discriminant models of blasts and seismic events in mine seismology," *Int. J. Rock Mech. Mining Sci.*, vol. 86, pp. 282–291, Jul. 2016.
[28] L. J. Dong, J. Wesseloo, Y. Potvin, and X. B. Li, "Discrimination of mine seismic events and blasts using the Fisher classifier, naive Bayesian classifier and logistic regression," *Rock Mech. Rock Eng.*, vol. 49, no. 1, pp. 183–211, Jan. 2016.
[29] L. Dong and X. Li, "Comprehensive models for evaluating rockmass stability based on statistical comparisons of multiple classifiers," *Math. Problems Eng.*, vol. 2013, Sep. 2013, Art. no. 395096.

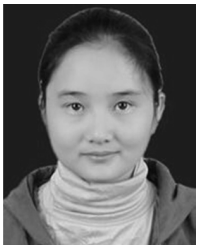

NAIPING LI received the M.M. degree in internal medicine from Central South University, Changsha, China, in 2013, where she is currently pursuing the Ph.D. degree. From 2012 to 2013, she was a Visiting Student with the Marshall Centre for Infectious Diseases Research and Training, The University of Western Australia, Perth, Australia. Her research interests include the diagnosis and treatment of hepatitis B, hepatitis C, and the pathological diagnosis of liver disease using artificial intelligence.

YONGFANG JIANG received the Ph.D. degree in internal medicine from Central South University, Changsha, China, in 2003. From 2012 to 2013, he was a Visiting Scholar with the School of Medicine, University of Colorado. His current research interests include the pathological diagnosis of liver disease. He has received two province-ministry level awards.

Dr. Jiang is a member of the Committee on Liver Disease of the Chinese Research Hospital Society and the Young Member of the Special Committee of Liver Disease of the Chinese Medical Association.

GUOZHONG GONG received the Ph.D. degree in internal medicine from Central South University, Changsha, China, in 2004. From 1998 to 2000, he was a Visiting Scholar with the School of Medicine, University of Colorado. He has authored over 40 academic papers. His current research interests include the diagnosis and treatment of hepatitis B and hepatitis C. He has received eight province-ministry level awards.

He is currently a Professor and the Director of the Institute of Hepatology, Central South University. He is the Committee Member of the Asian-Pacific Medical Bio-Immunology Society and the Standing Committee Member of the Hepatology Branch of the Asia-Pacific Medical Bio-Immunology Society. He was invited to serve as the Editorial Board Member of seven medical journals, including the *Chinese Journal of Infectious Diseases*, the *Journal of Central South University*—Medical Edition, and the *Journal of Practical Hepatology*.

GUANGJIE HAN (S'01–M'05) received the Ph.D. degree from Northeastern University, Shenyang, China, in 2004. From 2004 to 2006, he was a Product Manager with ZTE Company. He was a Post-Doctoral Researcher with the Department of Computer Science, Chonnam National University, Gwangju, South Korea, in 2008. From 2010 to 2011, he was a Visiting Research Scholar with Osaka University, Suita, Japan. He is currently a Professor with the Department of Information and Communication System, Hohai University, Changzhou, China. He has authored over 230 papers published in related international conference proceedings and journals. He holds 100 patents. His current research interests include sensor networks, computer communications, mobile cloud computing, and multimedia communication and security.

Dr. Han is a member of ACM. He received the Best Paper Award from the ComManTel 2014, ComComAP 2014, Chinacom 2014, and Qshine 2016. He has served as a co-chair for over 50 international conferences/workshops and as a technical program committee member of over 150 conferences. He has served on the Editorial Boards of up to 14 international journals, including the IEEE Access, *Telecommunication Systems*, the *International Journal of Ad Hoc and Ubiquitous Computing*, the *Journal of Internet Technology*, and *KSII Transactions on Internet and Information Systems*. He has guest edited a number of special issues in IEEE journals and magazines. He has served as a reviewer of over 50 journals.

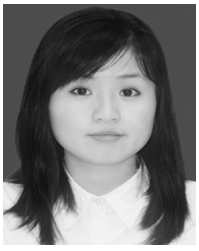

JING MA received the Ph.D. degree in internal medicine from Central South University, Changsha, China, in 2013. From 2012 to 2013, she was an International Visiting Exchange Scholar with Medical School, Yale University, New Haven, USA. She is currently an attending Physician with the Infectious Disease Department, Second Xiangya Hospital, Central South University. Her research interests include the diagnosis and treatment of hepatitis B and hepatitis.